OPEN ACCESS
CellPress

Cell Reports
Article

Dachsous-Dependent Asymmetric Localization of Spiny-Legs Determines Planar Cell Polarity Orientation in *Drosophila*

Tomonori Ayukawa,[1,2,3] Masakazu Akiyama,[4] Jennifer L. Mummery-Widmer,[5] Thomas Stoeger,[5,8] Junko Sasaki,[6,7] Juergen A. Knoblich,[5] Haruki Senoo,[2] Takehiko Sasaki,[1,3,6] and Masakazu Yamazaki[1,2,3,*]
[1]Research Center for Biosignal, Akita University, Akita 010-8543, Japan
[2]Department of Cell Biology and Morphology, Akita University Graduate School of Medicine, Akita 010-8543, Japan
[3]Global COE program, Gunma University and Akita University, Akita 010-8543, Japan
[4]Research Institute for Electronic Science, Hokkaido University, Hokkaido 060-0812, Japan
[5]Institute of Molecular Biotechnology of the Austrian Academy of Sciences (IMBA), Vienna 1030, Austria
[6]Department of Medical Biology, Akita University Graduate School of Medicine, Akita 010-8543, Japan
[7]Precursory Research for Embryonic Science and Technology, Japan Science and Technology Agency, Tokyo 102-0075, Japan
[8]Present address: Institute of Molecular Life Sciences, Irchel Campus, University of Zurich, Winterthurerstrasse 190, Zurich 8057, Switzerland
*Correspondence: yamazaki@med.akita-u.ac.jp
http://dx.doi.org/10.1016/j.celrep.2014.06.009

SUMMARY

In *Drosophila*, planar cell polarity (PCP) molecules such as Dachsous (Ds) may function as global directional cues directing the asymmetrical localization of PCP core proteins such as Frizzled (Fz). However, the relationship between Ds asymmetry and Fz localization in the eye is opposite to that in the wing, thereby causing controversy regarding how these two systems are connected. Here, we show that this relationship is determined by the ratio of two Prickle (Pk) isoforms, Pk and Spiny-legs (Sple). Pk and Sple form different complexes with distinct subcellular localizations. When the amount of Sple is increased in the wing, Sple induces a reversal of PCP using the Ds-Ft system. A mathematical model demonstrates that Sple is the key regulator connecting Ds and the core proteins. Our model explains the previously noted discrepancies in terms of the differing relative amounts of Sple in the eye and wing.

INTRODUCTION

The planar cell polarity (PCP) pathway coordinates cell polarization within an epithelial sheet in both vertebrates and invertebrates (Adler, 2002; Goodrich and Strutt, 2011; Gubb and García-Bellido, 1982; Simons and Mlodzik, 2008). In various tissues (Das et al., 2002; Goodrich and Strutt, 2011; Strutt et al., 2002; Strutt, 2001; Usui et al., 1999), PCP is established by the polarized localization of members of a "core" group of PCP proteins that includes the seven-pass transmembrane receptor Frizzled (Fz) (Gubb and García-Bellido, 1982; Vinson et al., 1989), the four-pass transmembrane protein Strabismus (Stbm; also known as Van Gogh; Taylor et al., 1998; Wolff and Rubin, 1998), and the seven-pass transmembrane cadherin Flamingo (Fmi; also known as Starry Night; Chae et al., 1999; Usui et al., 1999). In the *Drosophila* wing, the PCP core proteins are recruited to the opposite edges of each cell and assemble into asymmetric apicolateral complexes. Distal complexes are composed of Fz and the intracellular proteins Dishevelled (Dsh) and Diego (Dgo) (Axelrod, 2001; Feiguin et al., 2001; Shimada et al., 2001; Strutt, 2001), whereas proximal complexes involve Stbm and the cytoplasmic component Prickle (Pk) (Bastock et al., 2003; Jenny et al., 2003; Tree et al., 2002). Fmi appears in both proximal and distal complexes (Figure S1A; Usui et al., 1999). All the core proteins are required for the proper polarization of each core protein (Strutt, 2002), and this asymmetry generates distally pointing wing hairs at the distal vertex of the cell (Figure S1A; Adler, 2002; Goodrich and Strutt, 2011; Simons and Mlodzik, 2008). The asymmetry of the core proteins is regulated by intra- and intercellular feedback interactions between the distal and proximal complexes, which antagonize each other in the same cell and exhibit reciprocal localization (Amonlirdviman et al., 2005; Bastock et al., 2003; Das et al., 2004; Jenny et al., 2005; Tree et al., 2002). The distal and proximal complexes also interact to form complexes that straddle the proximodistal junctions between adjacent cells, leading to the local alignment of PCP complexes among small groups of cells (Figure S1A; Chen et al., 2008; Strutt and Strutt, 2008; Wu and Mlodzik, 2008). However, how the asymmetry of the core proteins is globally aligned along the proximal-distal (PD) axis of the wing remains unclear.

The atypical cadherin Dachsous (Ds) (Adler et al., 1998; Clark et al., 1995), Fat (Ft) (Mahoney et al., 1991; Matakatsu and Blair, 2004), and the Golgi kinase Four-jointed (Fj) (Ishikawa et al., 2008; Villano and Katz, 1995) are thought to be involved in core protein alignment, and expression gradients of Ds and Fj have been proposed as the global directional cues orienting core protein asymmetry (Ma et al., 2003; Yang et al., 2002). Ds and Ft use their extracellular domains to bind to each other at cell-cell boundaries (Brittle et al., 2010; Ma et al., 2003; Matakatsu and Blair, 2004; Simon et al., 2010), and this interaction

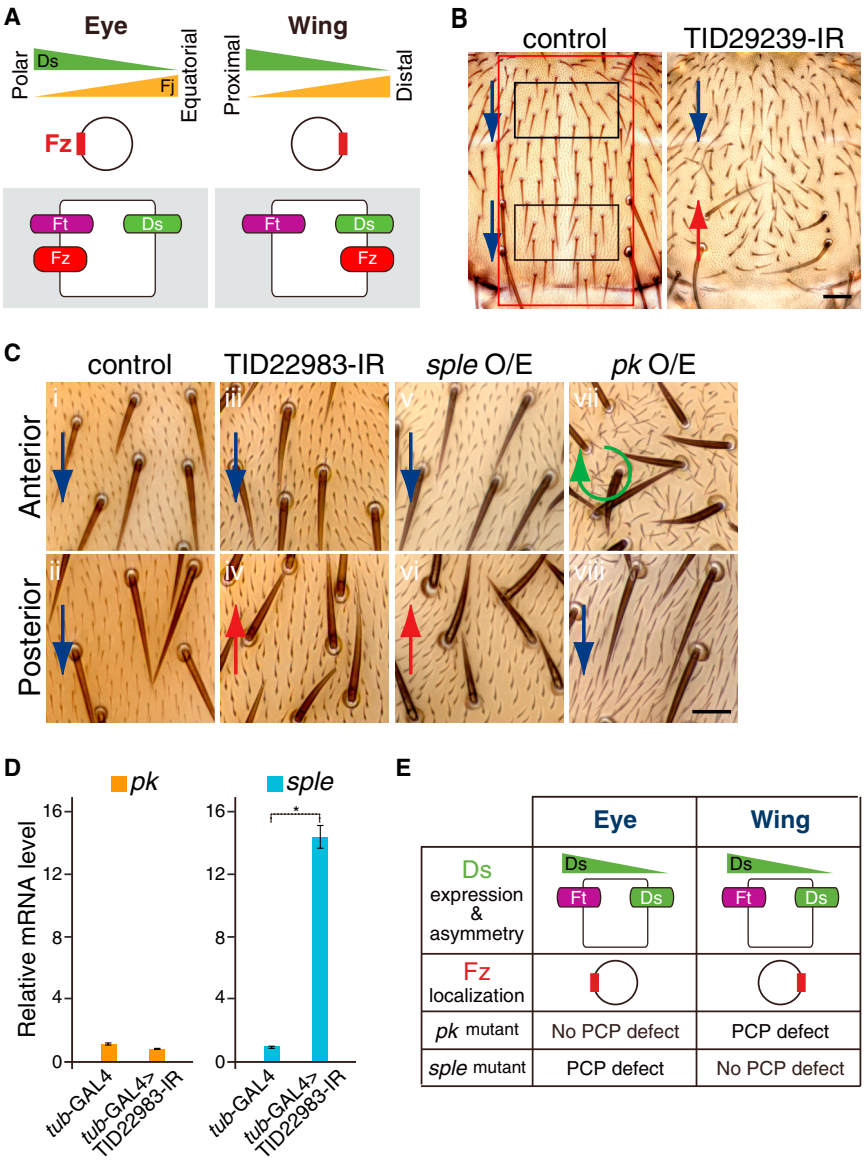

Figure 1. Overexpression of *sple* Leads to Reversed Polarity in the Posterior Notum

(A) (Top) Schematic diagram illustrating the relationship between the Ds and Fj gradients and the orientation of Fz localization in cells of the *Drosophila* eye and wing. Fz localization in eye R3 and R4 cells and in wing epithelial cells is shown in the schematic. (Bottom) Subcellular localization of Ds and Ft. The relationship of Ds/Ft localization to Fz localization is opposite between the eye and wing.

(B) Bristle phenotype on the notum in *pnr*-GAL4 (control) and *pnr*-GAL4 > UAS-TID29239-IR (TID29239-IR) transgenic *Drosophila*. The area of *pnr*-GAL4 expression is indicated by the red box in the control, with the top and bottom black boxes indicating the anterior and posterior regions of the notum, respectively. Normal (bristle tip pointing posteriorly) and reversed polarity are indicated by the blue and red arrows, respectively. The scale bar represents 100 μm.

(C) Orientation of bristles and small epidermal hairs (trichomes) in the anterior and posterior notum regions (as outlined in B) in *pnr*-GAL4 (control; i and ii), *pnr*-GAL4 > UAS-TID22983-IR (TID22983-IR; iii and iv), *pnr*-GAL4 > UAS-*sple* (10×UAS, attP2; *sple* O/E; v and vi), and *pnr*-GAL4 > UAS-*pk* (10×UAS, attP2; *pk* O/E; vii and viii) flies. Normal, reversed, and abnormal polarities are indicated by blue, red, and green arrows, respectively. The scale bar represents 20 μm.

(D) qRT-PCR analysis of *pk* and *sple* expression in *tub*-GAL4 (control) and *tub*-GAL4 > UAS-TID22983-IR pupae. Values were normalized to the mRNA level of the housekeeping gene *RpL32* and are expressed relative to the control. Data are the mean ± SE (n = 3). *$p < 0.01$.

(E) Table illustrating the postulated correlations between Fz localization relative to the Ds/Fj gradients (the Ds/Ft asymmetries) and the responsible Pk isoform in the *Drosophila* eye and wing.

is modulated by phosphorylation of the Ds and Ft extracellular domains by Fj (Brittle et al., 2010; Ishikawa et al., 2008; Simon et al., 2010). Fj-mediated phosphorylation increases the ability of Ft to interact with Ds but decreases the ability of Ds to bind to Ft. Thus, imbalances in the Ds and/or Fj levels between adjacent cells create subcellular asymmetries in Ds and Ft across cells, with Ds and Ft localizing at opposite sides of each cell (Figure S1B; Ambegaonkar et al., 2012; Brittle et al., 2012). Herein, we will refer to such imbalances between adjacent cells and asymmetries as Ds/Fj imbalances (or simply Ds imbalance) and Ds/Ft asymmetries (or simply Ds asymmetry), respectively.

Recent reports demonstrate that Ds imbalance directs asymmetric growth of microtubules from concentrations of high Ds to low Ds, leading to biased transport of Fz-containing vesicles in the wing (Harumoto et al., 2010; Shimada et al., 2006). However, the proposal that Ds/Fj imbalances are mediators of the global directional cues has been controversial. Although differences in expression of Ds and Fj in adjacent cells function as directional cues in the eye, such differences are at least partially dispensable in the wing, because simultaneous uniform expression of Ds and Fj rescues most of the PCP defects of the *ds* and *fj* double mutant in the wing, but not in the eye (Matakatsu and Blair, 2004; Simon, 2004). In addition, the Ds-Ft system does not act directly upstream of the PCP core proteins in the *Drosophila* abdomen (Casal et al., 2006). Recently, it has been proposed that, in the wing, the Ds-Ft system contributes to the global alignment of the core proteins along the PD axis, probably not by creating subcellular asymmetries in Ds and Ft but by regulating mechanical forces and cell rearrangements (Aigouy et al., 2010).

The intricacy of the molecular mechanisms underlying the global PCP pattern is also highlighted by the fact that the orientation of the Fz localization relative to the Ds/Fj gradients (the Ds/Ft asymmetries) in the *Drosophila* wing is opposite to the orientation of the Fz localization in the eye (Figure 1A;

Ma et al., 2003; Wu and Mlodzik, 2009; Yang et al., 2002). The conflicting pattern in the eye and wing has been one of the major barriers to understanding how the Ds-Ft system and the PCP core protein asymmetries are connected.

RESULTS

Overexpression of *sple* Leads to Reversed Polarity in the Posterior Notum

In *Drosophila*, the sensory bristles on the notum normally point to the posterior, and mutations in PCP genes disrupt this orientation. We previously performed a tissue-specific genome-wide screen of a transgenic RNAi library from the Vienna *Drosophila* RNAi Center and identified a group of genes whose knockdown resulted in prominent defects in bristle orientation (Mummery-Widmer et al., 2009). In the RNAi lines *oatp30B* (transformant ID [TID] 22983 or TID22984) and *pncr003:2L* (TID29239), a reverse orientation of the bristles and small epidermal hairs (trichomes) was observed in the posterior region of the notum (Figures 1B and 1Ci–1Civ; data not shown). However, when we attempted to confirm the involvement of these two genes in PCP using a different set of RNAi lines, no reversed PCP phenotype was observed (data not shown). Therefore, we examined the transgene insertion sites in the TID22983, TID22984, and TID29239 lines and found that they were all identical and 2 bp upstream of exon 3 of the *pk* gene (Figure S1C). The *pk* gene encodes three isoforms, *pk*, *sple*, and *pkM* (Gubb et al., 1999). The *pk* and *sple* isoforms are involved in PCP, but *pkM* is only expressed at the embryonic stage and has no known function (Gubb et al., 1999). Using quantitative real-time RT-PCR (qRT-PCR), we examined *pk* transcripts in pupae, in which expression of the TID22983-IR transgene was driven by *tubulin* (*tub*)-GAL4. Transcripts of *sple*, but not *pk*, were significantly increased in flies showing reversed bristle orientation (Figure 1D). The reversed PCP phenotype induced by all the upstream activating sequence (UAS)-IR lines was observed only when crossed with the GAL4 line (data not shown), and consistently, the increased expression of *sple* did not appear to be tissue specific (Figure S1D). These data suggest the involvement of *sple* in the PCP reversal phenotype.

When we used a site-specific integration technique (Groth et al., 2004) to insert a *sple* or *pk* transgene into the same chromosomal position (attP2), overexpression of *sple*, but not *pk*, phenocopied the reversed polarity observed in the RNAi lines (Figures 1Cv–1Cviii). Identical results were obtained when the *pk* or *sple* transgene was inserted at attP33 or attP40 (data not shown). Thus, increased *sple* expression may be responsible for the PCP reversal phenotype. Intriguingly, *pk* overexpression had a reciprocal effect, altering bristle and trichome orientation in the anterior notum (Figures 1Cvii and 1Cviii), as observed in the abdomen (Lawrence et al., 2004). These observations prompted us to examine the functional differences between Pk and Sple in PCP regulation.

Pk and Sple Expression Levels Differ between the *Drosophila* Eye and Wing

The Pk and Sple proteins both contain three LIM domains and a prickle espinas testin domain but differ in their N-terminal domains (Figure S1E). The *pk* isoform-specific mutants, pk^{pk} and pk^{sple}, exhibit PCP defects in reciprocal regions of the *Drosophila* body (Gubb et al., 1999). The pk^{pk} mutant shows a strong PCP defect in the wing, but not the eye, whereas the pk^{sple} mutant shows a prominent PCP defect in the eye, but not the wing (Figure 1E). Such reciprocity also exists for the relationship between the Ds/Fj gradients (the Ds-Ft asymmetries) and the Fz localization, which are also opposite in the eye and wing (Figure 1A; Adler et al., 1998; Casal et al., 2006; Ma et al., 2003; Strutt and Strutt, 2002; Wu and Mlodzik, 2009; Yang et al., 2002). In addition, a recent report found that the responsiveness to the global cues is altered in the wing of the pk^{pk} mutant (Hogan et al., 2011). Whereas these data may imply that Pk isoforms are involved in global patterning, an interpretation for this phenotype was not proposed, and the molecular mechanism underlying the phenotype remains unknown.

We hypothesized that these differences between the eye and wing were due to the distinct levels of *pk* and *sple* expression in the eye and wing. Therefore, we examined the expression of endogenous *pk* and *sple* in the wild-type *Drosophila* eye and wing. The mRNA levels of *pk* and *sple* were strikingly different between the eye and wing. Whereas *pk* and *sple* expression levels were similar in the larval eye disc and the pupal eye, the level of *pk* mRNA was markedly higher than that of *sple* mRNA in the larval wing disc and the pupal wing (Figure 2A). These results implied that the relative levels, or the ratio, of Pk and Sple expression might be a determining factor in the relationship between the Ds/Ft asymmetries and the orientation of the Fz localization.

The Levels and/or Ratio of Pk and Sple Expression Determines Core Protein Localization Relative to the Ds/Ft Asymmetries

We hypothesized that *sple* overexpression in the wing would mimic the PCP status of the eye by changing the *pk*:*sple* ratio and would therefore cause PCP reversal (Figure S2A). Consistent with this hypothesis, *sple* overexpression reversed the orientation of wing hairs (Figure 2B). Although *sple* overexpression has been previously associated with a reversal in hair polarity (Gubb et al., 1999; Lee and Adler, 2002), the following points remain unclear: (1) whether a *sple* expression level equivalent to that of *pk*, as is observed in the eye, is sufficient to reverse the polarity in the wing and (2) whether the orientation of the core protein asymmetry is also reversed upon *sple* overexpression. The overexpression of *sple* in the TID22983 line caused the *pk*:*sple* ratio in the wing to become equivalent to that in the wild-type eye and reversed the hair polarity, indicating successful reconstitution of the PCP status of the eye in the wing (Figures 2B and 2C). In addition, the orientation of core protein localization was also reversed upon *sple* overexpression (Figure 2D). Similar results were achieved using other UAS-*sple* constructs. In the presence of large amounts of *sple*, due to *sple* expression driven by 5× or 10× UAS sites, hair orientation was reversed (Figures 2B, 2C, and S2B), but orientation was normal in the presence of 1× UAS-*sple* expression (Figure 2C). The same PCP reversal phenotype was observed using other GAL4 lines (Figures S2C and S2D; see Supplemental Results and Figure S2F). Importantly, *sple* overexpression did not affect

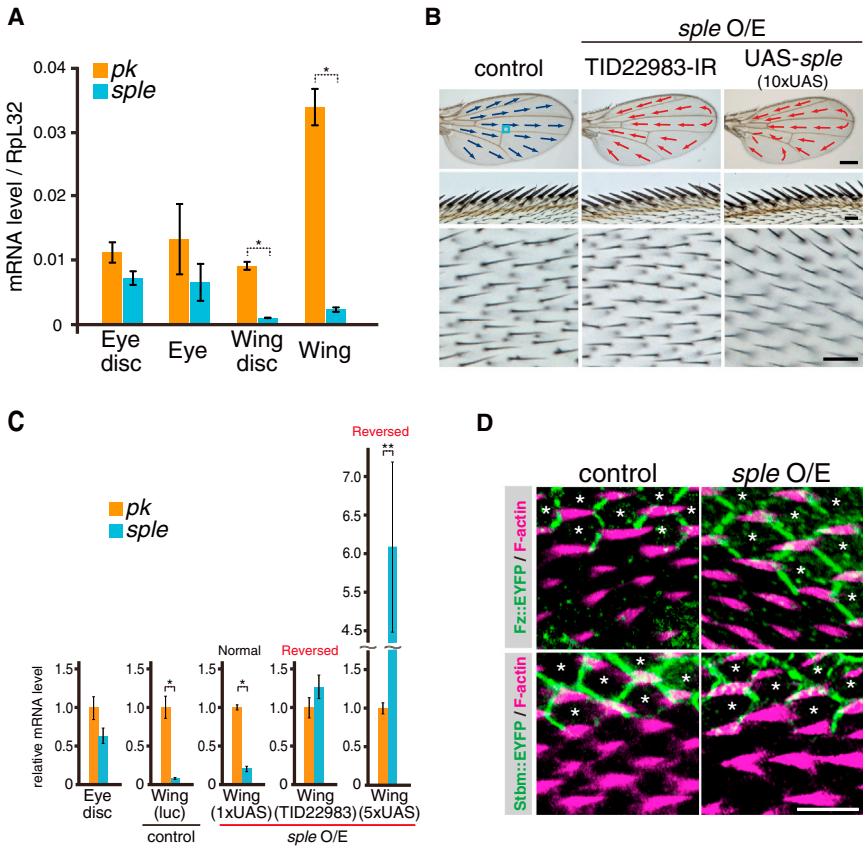

Figure 2. The Pk:Sple Ratio Differs between the *Drosophila* Eye and Wing and Determines PCP Core Protein Localization Relative to Ds/Ft Localization

(A) Quantitative RT-PCR of *pk* and *sple* levels in larval eye and wing discs and pupal eyes and wings from wild-type *Drosophila* analyzed as described in Figure 1D. Data are the mean ± SE (n = 3). *p < 0.05.

(B) Orientation of hairs on the dorsal surface of the wing in *scalloped* (*sd*)-GAL4 > UAS-luciferase (10×UAS, attP2; control), *sd*-GAL4 > UAS-TID22983-IR (TID22983-IR), and *sd*-GAL4 > UAS-*sple* (10×UAS, attP2; UAS-*sple*) flies. Top panels: arrows indicate the orientation of wing hairs (blue, normal polarity; red, reversed polarity; distal is to the right). Middle panels: portion of the wing margin showing normal and reversed polarity bristles. Bottom panels: high-magnification images showing the area of the wing delineated by the box in the control wing (top panel). The scale bars represent 300 μm (top panels) or 20 μm (middle and bottom panels).

(C) qRT-PCR of *pk* and *sple* expression in the eye discs of the wild-type larvae in (A) and in the wings of *sd*-GAL4 > UAS-luciferase (luc; control), *sd*-GAL4 > 1×UAS-*sple* (attP2; 1×UAS), *sd*-GAL4 > UAS-TID22983-IR (TID22983), and *sd*-GAL4 > 5×UAS-*sple* (attP2; 5×UAS) pupae. Data were analyzed as described in Figure 1D, and the means ± SE (n = 3) are shown. *p < 0.01, **p < 0.05.

(D) Localization of clonally expressed Fz::EYFP and Stbm::EYFP at 31 hr APF in wings of a control pupa and a *sple*-overexpressing pupa (EYFP, green; F-actin, magenta). White asterisks indicate cells expressing Fz::EYFP or Stbm::EYFP. The scale bar represents 5 μm.

the expression patterns of Ds or Fj (Figure S2E). Taken together, our data demonstrate that the relative levels of Pk and Sple (the ratio of Pk to Sple expression) govern the relationship between the Ds-Ft system and the Fz asymmetry orientation.

Pk and Sple Have Mutually Antagonistic Functions and Form Different Complexes

The importance of the Pk and Sple levels, and/or the balance between them, was previously demonstrated in *Drosophila* tissues (Gubb et al., 1999). To analyze in detail the relationship between Pk and Sple during PCP establishment, we produced a series of transgenic flies simultaneously overexpressing defined levels of *pk* and/or *sple* via vectors bearing different numbers of UAS sites (1×, 3×, or 5×; Pfeiffer et al., 2010). Using site-specific integration (Groth et al., 2004; Pfeiffer et al., 2010), we achieved several combinations of *pk* and *sple* expression levels and found that the PCP reversal associated with *sple* overexpression could be suppressed by *pk* in an expression-level-dependent manner (Figures 3A and 3B). These results strongly support the hypothesis that the relative Pk and Sple levels determine the PCP orientation relative to the Ds/Ft asymmetries.

To investigate the mechanism underlying the mutual antagonism of Pk and Sple, we examined their subcellular localization patterns in the pupal wing. Consistent with a previous report (Tree et al., 2002), clonally expressed enhanced GFP (EGFP)::Pk was localized at the proximal edge of each wing cell in control flies (Figure 3C, left). By contrast, clonally expressed EGFP::Sple was localized at the distal edge in control wing cells and resulted in reversed hair polarity (Figure 3C, middle; Strutt et al., 2013). Upon overexpression of untagged Sple, EGFP::Pk was recruited to the distal cell edge (Figure 3C, right), the opposite of its normal localization.

Although these data indicate that Pk localization in the pupal wing cells can be reversed by altering the Pk:Sple ratio, it is still unclear when or how Pk localization is affected because, in this experimental system, Sple is already overexpressed prior to the pupal stage. In addition, PCP domains are already established in the larval wing disc and are then reorganized in the pupal stage by first decreasing and then increasing the magnitude of the PCP domains (Aigouy et al., 2010; Classen et al., 2005). We examined if the Pk localization can be reversed by *sple* overexpression in the larval wing disc. Clonally expressed EGFP::Pk was localized away from the center of the wing pouch, as reported previously (Sagner et al., 2012), whereas EGFP::Sple was localized toward the center of the wing pouch (Figures S3D, S3D', S3E, and S3E'; see also Figures S3A–S3C). As in the pupal wing, when untagged *sple* was overexpressed, EGFP::Pk was recruited to the side of the cell opposite its normal localization,

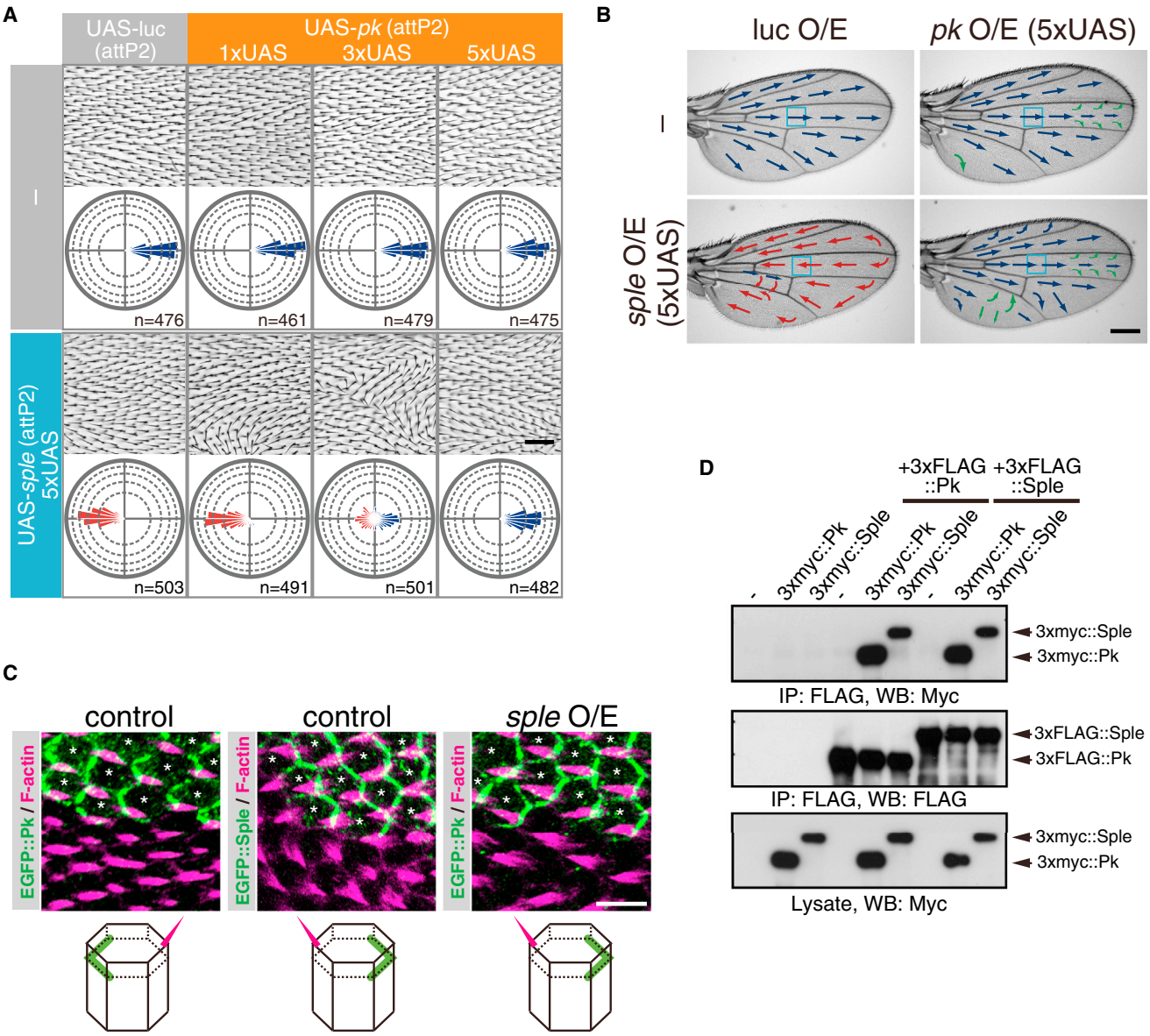

Figure 3. Pk and Sple Have Mutually Antagonistic Functions and Form Different Complexes

(A) Polarity changes associated with simultaneous overexpression of various combinations of *pk* and *sple* (driven by *sd*-GAL4) in the *Drosophila* wing. For each genotype, the upper panel shows hairs on the dorsal surface of the adult wing from the region boxed in (B) and the lower panels are rose diagrams composed of 36 bins of 10° each showing the angular distribution of wing hairs. The concentric circles in each rose diagram indicate 10% increments. The total number of wing hairs analyzed from three adult wings per group (n) is indicated at the lower right of each panel. The scale bar represents 40 μm.

(B) Wing hair polarity changes in adult wings overexpressing luciferase (luc O/E; control), *pk*, *sple*, or *pk* plus *sple* (driven by *sd*-GAL4). Distal, proximal, and abnormal polarities on the dorsal wing surface are indicated by blue, red, and green arrows, respectively. The scale bar represents 300 μm.

(C) Top panels: localization of clonally expressed EGFP::Pk (left) and clonally expressed EGFP::Sple (middle) in wings of control pupae and clonally expressed EGFP::Pk (right) in wings of a *sple*-overexpressing pupa, at 31 hr APF. EGFP, green; F-actin, magenta. White asterisks indicate cells expressing EGFP::Pk or EGFP::Sple. The scale bar represents 5 μm. Bottom panels: schematic diagrams illustrating the localization of EGFP::Pk or EGFP::Sple (green) and the wing hair orientation (magenta).

(D) Immunoprecipitation (IP) and western blot (WB) analysis of tagged Sple and Pk in human embryonic kidney 293 cells. Pk and Sple exhibit both homophilic and heterophilic interactions.

indicating that Sple overexpression is effective in changing Pk localization in the larval stage (Figures S3F and S3F'). Recently, Sple induction using hs-GAL4 during the pupal stage was reported to change hair polarity in the wing, and this induction was effective until 28 hr after puparium formation (APF) (Doyle et al., 2008; see below). These results suggested that Pk localization can be reversed by the Pk:Sple ratio both in the larval wing disc and in the pupal wing.

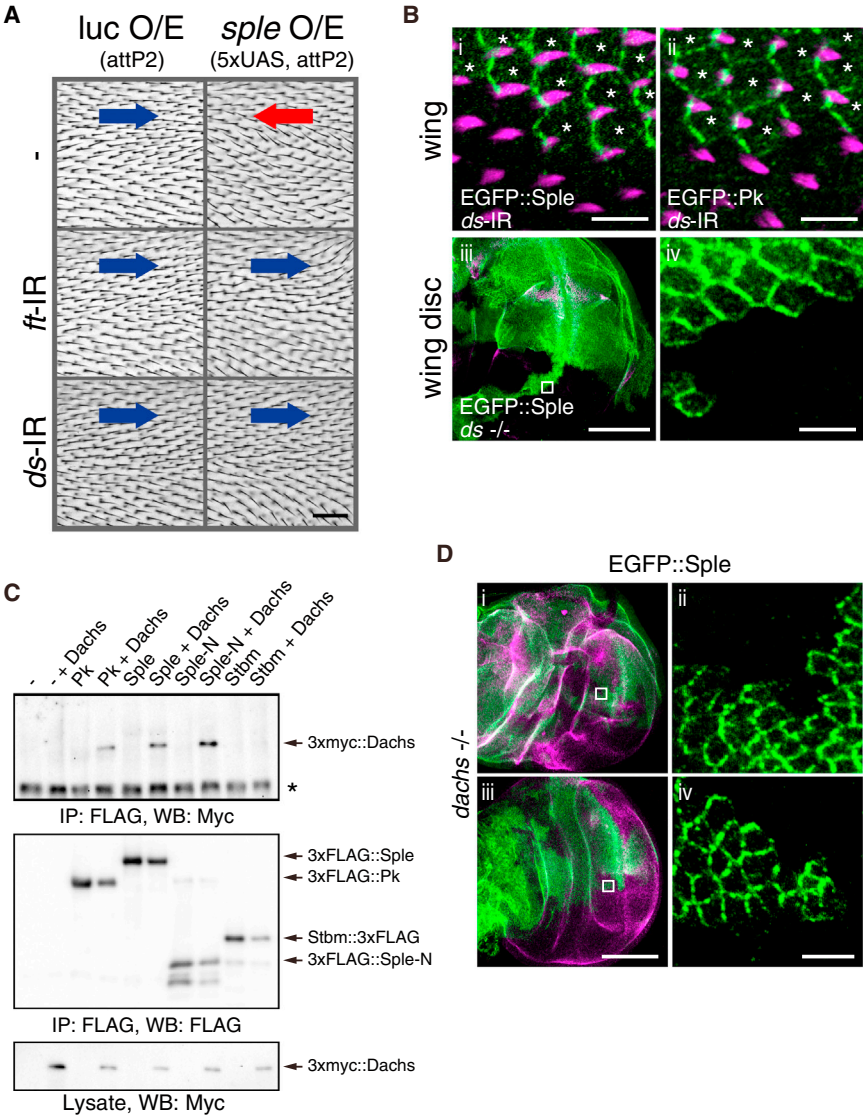

Figure 4. Ds Group Proteins Polarize Sple at the Cell Edge with the Highest Ds Level

(A) Orientation of hairs on the dorsal surface of wings at the same region as boxed in Figure 3B in luciferase-expressing (luc O/E; control) flies or *ds* or *ft* knockdown flies (*ds*-IR and *ft*-IR) overexpressing *sple* (*sple* O/E). Normal and reversed polarity are indicated by the blue and red arrows, respectively. The scale bar represents 40 μm.

(B) Localization of clonally expressed EGFP::Sple and EGFP::Pk at 31 hr APF in wings in which *ds* is knocked down (i and ii). White asterisks indicate cells expressing EGFP::Sple or EGFP::Pk (i and ii). Localization of clonally expressed EGFP::Sple in the wing disc of the ds^{UA071}/ds^{38K} mutant (iii and iv). High magnification of the boxed region in (iii) is shown in (iv). EGFP, green; F-actin (i and ii) and Delta (iii), magenta. The scale bars represent 5 μm (i, ii, and iv) or 100 μm (iii).

(C) Coimmunoprecipitation analysis showing that FLAG-tagged Dachs interacts with myc-tagged Pk, Sple, and Sple-N, but not Stbm. Asterisk indicates the immunoglobulin G bands.

(D) Localization of clonally expressed EGFP::Sple in the wing disc of the *dachs* mutant (i and ii: d^1/d^{GC13}; iii and iv: d^1/d^{210}). High magnification of the boxed regions in (i) and (iii) are shown in (ii) and (iv), respectively. EGFP, green; Delta, magenta. The scale bars represent 100 μm (i and iii) or 5 μm (ii and iv).

To understand the molecular mechanism underlying the reversal of Pk localization by *sple* overexpression, we performed cotransfection experiments. Pk and Sple can form both heterophilic and homophilic complexes (Figure 3D). These results are consistent with a previous report demonstrating homophilic interactions between C-terminal fragments of Pk in an in vitro experiment (Jenny et al., 2003). Taken together, these data suggest that Pk and Sple physically interact with each other and with themselves, have mutually antagonistic functions, and form a variety of complexes with distinct subcellular localizations.

The Ds-Ft System Is Required for Sple-Mediated PCP

What triggers Sple (or a protein complex containing Sple) to localize at the opposite side of each cell compared to Pk localization? A potential candidate is the complex containing the atypical cadherin Ds and Ft. PCP reversal by *sple* overexpression was suppressed by knockdown of *ds* or *ft* (Figure 4A). This finding is in line with a recent report showing that reduced activity of Ds/Ft pathway genes modifies the wing hair polarity defect in the pk^{pk} mutant, in which *sple*, but not *pk*, is expressed at the endogenous level (Hogan et al., 2011). Next, we examined the localization of Sple in the pupal wing where *ds* expression is diminished. Owing to the strong PCP defect in the pupal wing of the *ds* mutant, we used pupal wings in which *ds* was knocked down. The localization of EGFP::Sple was changed from distal to proximal in the *ds* knockdown pupal wing (Figure 4Bi). By contrast, Pk localization in the pupal wing was not affected by *ds* knockdown (Figure 4Bii), similar to previous results showing almost normal Pk localization in the wing disc of a *ds* mutant (Sagner et al., 2012). Additionally, in the *ds* mutant wing disc, the localization pattern of EGFP::Sple was changed from toward to away from the center of the wing pouch, resulting in the same localization as Pk (Figures 4Biii and 4Biv; compare to Figures S3D' and S3E'). These results show that the Ds-Ft system is required for the localization and function of Sple for PCP formation.

The distal cell edge, where Sple is localized, appears to exhibit a high Ds level (Figure S1B); therefore, we investigated whether Sple can interact with Ds. Cotransfection experiments demonstrated that the N-terminal unique region of Sple (Sple-N) bound to the intercellular domain (ICD) of Ds, but not to that of Ft (Figure S4A). To identify the region of Sple responsible for the interaction with Ds-ICD, we produced a series of deletion fragments

of Sple-N (Figure S4B) and examined the interaction of these fragments with Ds-ICD. All the fragments containing the N-terminal region of Sple-N, but not the fragment lacking this region (Sple-NΔN), interacted with Ds-ICD, suggesting that the N-terminal region of Sple-N is sufficient for the interaction with Ds (Figure S4C). Using the same strategy, we also found that the middle (M) region of Ds-ICD is responsible for the interaction with Sple-N (Figures S4D and S4E).

Whereas these findings suggest that Sple-Ds cooperation polarizes Sple at the cell edge with the highest Ds level, other components may be involved in the process of Sple polarization because full-length Sple failed to interact with Ds-ICD in our experimental conditions (data not shown). Therefore, we focused on another Ds-Ft group protein, the atypical myosin Dachs, which interacts and colocalizes with Ds (Bosveld et al., 2012; Mao et al., 2006; Rogulja et al., 2008). Coimmunoprecipitation demonstrated that full-length Sple, as well as Sple-N, interacted with Dachs (Figure 4C). Consistent with this binding, the reversed localization of Sple was suppressed by loss of *dachs* in the wing disc (Figure 4D), resulting in the same localization as Sple in the *ds* mutant wing disc (Figure 4Biv). Interestingly, Pk also exhibited a weak interaction with Dachs (Figure 4C), and these two genes interacted genetically (Figure S4F), indicating that Pk is involved in a Dachs-mediated biological process via an unknown mechanism (see Discussion). Taken together, these results demonstrated that the localization and function of Sple is regulated through its interaction with Ds group proteins.

A Mathematical Modeling of Global PCP Patterning

To better understand the role of the Pk:Sple ratio in the PCP-signaling pathway, we developed a mathematical model to describe global PCP patterning. Our model includes two main processes important for PCP formation (see Supplemental Procedure for Mathematical Model for more detail). In brief, the first process is local cell-cell communication that is regulated by interactions between the distal (Fz-containing) and proximal (Stbm-containing) complexes on adjacent cells and the repulsive reaction between these complexes within cells. We call this "LOCAL" rule. The second process is the Ds-dependent global PCP regulation, which we call the "GLOBAL" rule (see also Figures S6A and S6B). We tested the applicability of this mathematical model for analyzing global PCP patterning by simulating PCP using the LOCAL and/or the GLOBAL rules. Simulations successfully reproduced many aspects of PCP in the wing (Supplemental Results; Figure S5; Movies S1 and S2).

Simulations Show the Importance of Sple in Global PCP Patterning

Recent studies revealed that PCP in the wing develops through complex events during the larval and pupal stages, by changing the PCP orientation and by decreasing and then increasing its magnitude (Aigouy et al., 2010; Sagner et al., 2012). This complexity makes it difficult to simulate the entire process of PCP in the *Drosophila* wing. In the following simulations, we aimed to recapitulate PCP in the wing at 20 hr APF because, after this time period, the global orientation of PCP is stable and its intensity simply increases (Aigouy et al., 2010). In the wild-type pupal wing at 20 hr APF, Fz is slightly localized distally, whereas Stbm is weakly polarized proximally in each wing cell (Aigouy et al., 2010). Taking the Fz and Stbm localization into account, we used an initial condition where both the Fz and Stbm complexes are slightly biased in opposite directions along the PD axis (Figure S6C; see also Supplemental Procedure for Mathematical Model) and performed simulations of PCP using both the LOCAL and GLOBAL rules (Equations 3, 4, 10, and 11 in Supplemental Procedure for Mathematical Model). These simulations reproduced the PCP status of the wild-type wing where Fz complexes in all cells are oriented toward the distal direction (Figures 5A, 5Bi, 5Bii, and S7A; Movie S3), and conversely, Stbm complexes are oriented toward the proximal direction (data not shown). Interestingly, in this case, without the Ds-dependent GLOBAL rule (the second terms of Equations 10 and 11 in Supplemental Procedure for Mathematical Model), PCP can be formed along the PD axis of the wing due to the initial bias of the Fz and Stbm complexes alone (Figures 5Biii, 5Biv, and S7B). This result supports the previous experimental results that the core protein asymmetries in the larval wing disc nearly obviate the need for Ds (Sagner et al., 2012) and that flattering the expressions of Ds and Fj still allows almost normal PCP in the wing (Matakatsu and Blair, 2004; Simon, 2004). Next, we tested whether our model can reproduce the reversed PCP phenotype by overexpressing *sple* in the wing. The orientation of PCP was reversed in our simulation simply by increasing the amount of Sple (Figures 5Bv, 5Bvi, and S7A; Movie S4). Consistent with our experimental results (Figures 2C and 3A), the presence of a large amount of Sple resulted in the reversed PCP phenotype (Figure S7D), whereas an increase in the amount of Pk did not affect PCP in the simulations (Figure S7C).

Next, we employed this mathematical model to analyze the phenotypes obtained by the induction of *sple* overexpression under several conditions and explored the unknown mechanism underlying these phenotypes. Ds is expressed at high levels in the proximal wing at 5 hr APF, and strong Ds expression extends into the distal region along the L3 vein by 17 hr APF (Figures 5Ci and 5Cii; Ma et al., 2003; Matakatsu and Blair, 2004), which produces symmetric gradients of Ds expression along the anterior-posterior (AP) axis (Figure 5Cii; Hogan et al., 2011). Consistent with the Ds gradient along the AP axis, induction of *sple* overexpression at approximately 19 hr APF orients the wing hairs toward the higher Ds expression (the L3 vein; Doyle et al., 2008), and a similar phenotype caused by loss of *pk* is diminished by loss of the *ds* group genes (Hogan et al., 2011). Earlier induction of *sple* overexpression caused more striking phenotypes in hair polarity, and more importantly, this resulted in the opposite phenotype in hair orientation (Doyle et al., 2008; Figures 5Ciii, 5Civ, and S2Gi; see below in detail).

In wings where *sple* overexpression was induced at 20 hr APF, the wing hairs pointed distally (near the L3 vein), posterior-distally (anterior to the L3 vein), or anterior-distally (posterior to the L3 vein; Figure 5Cv). By contrast, in wings where *sple* overexpression was induced at 96 hr after egg laying (AEL) or 6 hr APF, the hairs pointed in a reversed manner compared to those in wings with later induction of *sple* (Figures 5Civ and S2Gi; compared to Figures 5Cv and S2Gii). To examine the mechanism underlying this phenotypic difference, we simulated Ds

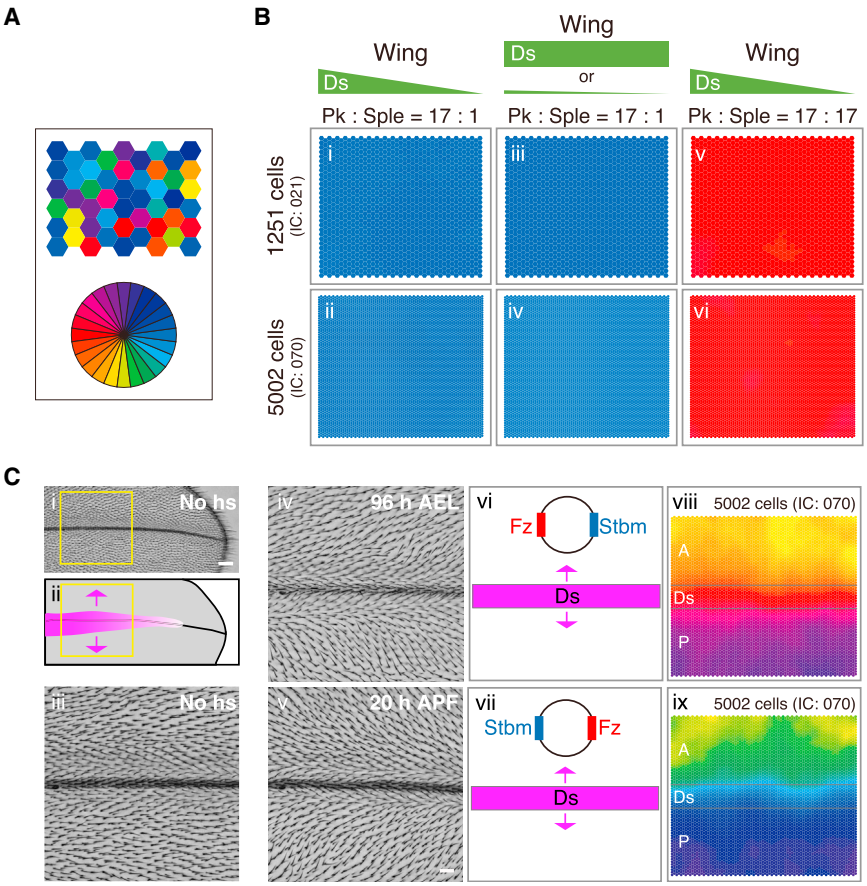

Figure 5. Numerical Simulations Support the Model that the Wing Utilizes Two Distinct Mechanisms for Global PCP Regulation and that Sple Is a Key Regulator for the Pathway that Is Involved in the Ds-Ft System

A representative result of the final states of 100 simulations in various conditions is shown in each panel. The information for the initial condition used in the simulation shown in the figure is at the left side of each panel (IC: three-digit number). See Supplemental Procedure for Mathematical Model for the parameter values used in the following simulations in this figure.

(A) In all simulations, each cell is represented by a hexagon. The orientation of the Fz asymmetric localization in each cell is demonstrated by different colors as shown in the colored circle.

(B) Simulation of wing PCP. A wild-type wing (i and ii), a wing in which the Ds expression pattern is flattened or diminished (iii and iv), and a wing overexpressing *sple* (v and vi) are shown. In all the simulations in (B), we used the same initial condition where the Fz complex is slightly distally biased, whereas Stbm complexes are slightly proximally biased (Figure S6C). Quantitative data are shown in Figure S7.

(C) Experimental and simulation results of *sple* overexpression at the indicated developmental stages. The distal part of the control adult wing (no hs, no heat-shock treatment, meaning *sple* overexpression was not induced; i) and a schematic diagram illustrating Ds expression in this region at approximately 17–26 hr APF (ii). Orientation of wing hairs in the region outlined in (i) in the control fly (iii) and in the flies where *sple* overexpression was induced at 96 hr AEL (iv) and at 20 hr APF (v). The initial Fz and Stbm localizations and the effect of Ds in simulations where *sple* overexpression was induced at 96 hr AEL (vi) and at 20 hr APF (vii; Figures S6C and S6D) and simulation results where *sple* overexpression was induced at 96 hr AEL (viii) and at 20 hr APF (ix) are shown at the right. The scale bars represent 60 μm (i) or 20 μm (iii–v).

expression along the L3 vein and its anterior and posterior regions and performed simulations (Figure 5Cvii; see Supplemental Procedure for Mathematical Model). Using initial conditions where the Fz complex localization is slightly distally biased and Stbm complexes are slightly proximally biased (Figures 5Cvii and S6C), we recapitulated the PCP phenotype of the wing in which *sple* overexpression was induced at 20 hr APF (Figure 5Cix). However, these conditions never produced the PCP pattern of wings in which *sple* overexpression was induced at 96 hr AEL (Figure 5Civ) or 6 hr APF (Figure S2Gi).

One possible explanation for this discrepancy may be a difference in the initial states of Fz and Stbm localization between these two time points, 20 hr APF and 96 hr AEL (or 6 hr APF). Pk localization is actually reversed by *sple* overexpression in the larval wing disc (Figure S3F'). Therefore, we examined the localization of the core protein Stbm in larval wing discs overexpressing *sple* and found that its localization was also reversed (Figures S3G, S3G', S3H, and S3H'). Using the reversed bias of Fz and Stbm localization as an initial condition (Figures 5Cvi and S6D), our simulations successfully recapitulated the PCP status of the wing where *sple* overexpression was induced at 96 hr AEL or 6 hr APF (Figure 5Cviii). These results suggest that the phenotypic differences induced by *sple* overexpression at distinct time points are caused by the distinct initial biases in the Fz and Stbm localization.

Given the importance of the reversed initial biases in the Fz and Stbm localization caused by *sple* overexpression during the early developmental stage, we resimulated PCP of the wing where *sple* is overexpressed, using these reversed biases as an initial condition. Accuracy of the Fz and Stbm alignment in these simulations was increased compared to those using the normal initial biases of Fz and Stbm localizations (compare Figure S7A [Movie S4] versus S7E [Movie S5] in the case of s = 1.42 or Figure S7D versus S7E in the case of s = 3.54 or 6.48). These results indicate that the initial biases (~20 hr APF) in the Fz and Stbm localization, as well as Ds-mediated global PCP regulation, are critical for PCP development during the pupal stage.

In addition to recapitulating the experimental results, we found an intriguing feature of *sple* overexpression clones in our simulations. In small clones, polarity inside the clones was never reversed (Figures 6Ai and 6Aii), but the PCP was reversed inside larger clones (Figures 6Aiii and 6Aiv). The same trend was detected in our experiments (Figures 6Bi and 6Bii). These results strongly support our hypothesis that Sple is a key regulator connecting the Ds-Ft system and the core proteins and that, when

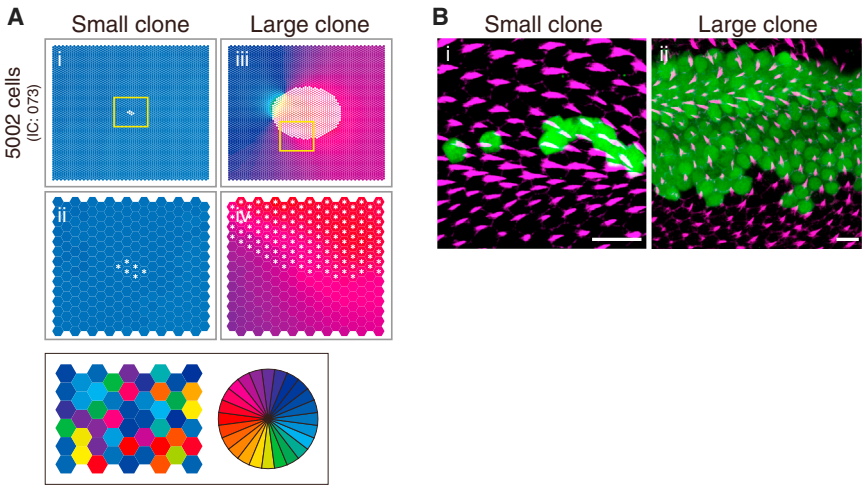

Figure 6. Prediction of Phenotypes of *sple* Overexpression Clones

(A) Simulation results of a small clone of cells overexpressing *sple* (i and ii) and a larger clone of cells overexpressing *sple* (iii and iv). ii and iv show high-magnification images of the boxed regions in (i) and (iii), respectively. Asterisks mark the cells overexpressing *sple*. The colored circle represents the direction of Fz localization in each cell, as in Figure 5.

(B) Experimental results showing a small clone (i) and a larger clone (ii) of wing cells overexpressing *sple*. The orientation of wing hairs at 31 hr APF in pupal wings clonally expressing EGFP plus untagged *sple* is shown. EGFP, green; F-actin, magenta. The scale bar represents 10 μm.

the amount of Sple is increased in the wing, Sple induces a reversal of PCP using the Ds-Ft system (see Supplemental Discussion).

DISCUSSION

The Pk:Sple Ratio Determines the Orientation of PCP Core Protein Localizations Relative to Ds/Ft Asymmetries in the Wing and Eye

The orientation of Fz localization relative to the Ds/Fj gradients (the Ds/Ft asymmetries) in the *Drosophila* wing is opposite to Fz orientation in the eye. This observation has been a puzzle in the PCP field and a barrier to understanding how the Ds-Ft system and PCP core protein asymmetries are connected. Our experiments and computational simulations have demonstrated that it is the Pk:Sple ratio that governs the relationship between the Ds/Ft asymmetries and core protein localization in the *Drosophila* eye and wing (Figures 1A, 2, 5, and 6). Importantly, our model is supported by a loss-of-function experiment in the eye from a previous study. The pk^{sple} mutant, which shows specific loss of the Sple isoform, exhibits a polarity reversal in the orientation of the eye ommatidia (Gubb et al., 1999; Strutt et al., 2013). The pk^{pk} mutant does not exhibit a complete reversal of PCP in the wing (Gubb et al., 1999), perhaps because the remaining endogenous amount of Sple is small (Figure 2A) and/or the timing of expression of endogenous *sple* is altered. These data reinforce the conclusion that skewing the Pk:Sple ratio alters PCP establishment in the wing and eye (see Supplemental Discussion; Olofsson et al., 2014).

A Possible Mechanism by which the Pk:Sple Ratio Determines the Orientation of the Core Proteins Relative to the Ds/Ft Asymmetries

We hypothesize that tissues in which Sple complexes (Sple-Pk and Sple-Sple) are predominant will tend to have one polarity, whereas tissues containing mainly Pk complexes will show the opposite polarity (Figure 7). However, we cannot exclude the possibility that uncomplexed Pk and Sple molecules may influence PCP determination even if Pk-Pk, Sple-Pk, and Sple-Sple complexes localize asymmetrically in each cell. Alternatively, multimeric protein complexes containing multiple Pk and/or Sple molecules may be responsible for establishing PCP.

Here, we found that, in tissues where Sple was relatively abundant, Sple (or the Sple complex) was recruited at the cell edge exhibiting the highest Ds level. Furthermore, biochemical and genetic experiments suggested a model in which Sple-Ds cooperation polarizes Sple (or Sple complexes) at the cell edge exhibiting the highest Ds level (Figure 7). We also demonstrated that the atypical myosin Dachs is heavily involved in the process of Sple polarization in the wing (Figure 4D; Supplemental Discussion). This observation is intriguing because *dachs* loss of function does not show a PCP defect as strongly as that of *ds* or *ft* loss of function in *Drosophila* tissues and Dachs does not appear to be as important to PCP in the eye as in the wing (Mao et al., 2006; Matakatsu and Blair, 2008). There may be a redundant unknown mechanism responsible for Sple asymmetry.

Intriguingly, in the wing of the pk^{pk} mutant, loss of *lowfat* (*lft*), one of the members of the Ds-Ft group, affects wing hair polarity in a manner similar to loss of *ds* or *ft* (Hogan et al., 2011). This is despite the fact that, in contrast to the *ds* or *ft* mutant, the *lft* mutant does not show any PCP defect in *Drosophila* tissues including the wing and eye (Mao et al., 2009). These observations are consistent with our result showing that Dachs is involved in Sple asymmetry. These results have profound implications regarding the relationship between Pk isoforms and the Ds-Ft system. In addition, our study revealed that Pk physically and genetically interacts with Dachs (Figures 4C and S4F), even though the subcellular localizations of these two proteins are opposite. There are several possibilities to explain the physiological relevance of the Pk-Dachs interaction. For example, Pk and Sple-Dachs complexes may have mutually antagonistic functions at the opposite cell edges, which is similar to the relationship between Pk (which is localized at the proximal cell border) and Dsh and Dgo (which are localized distally; Jenny et al., 2005). To understand the molecular mechanism governing global PCP patterning, it will be important to elucidate

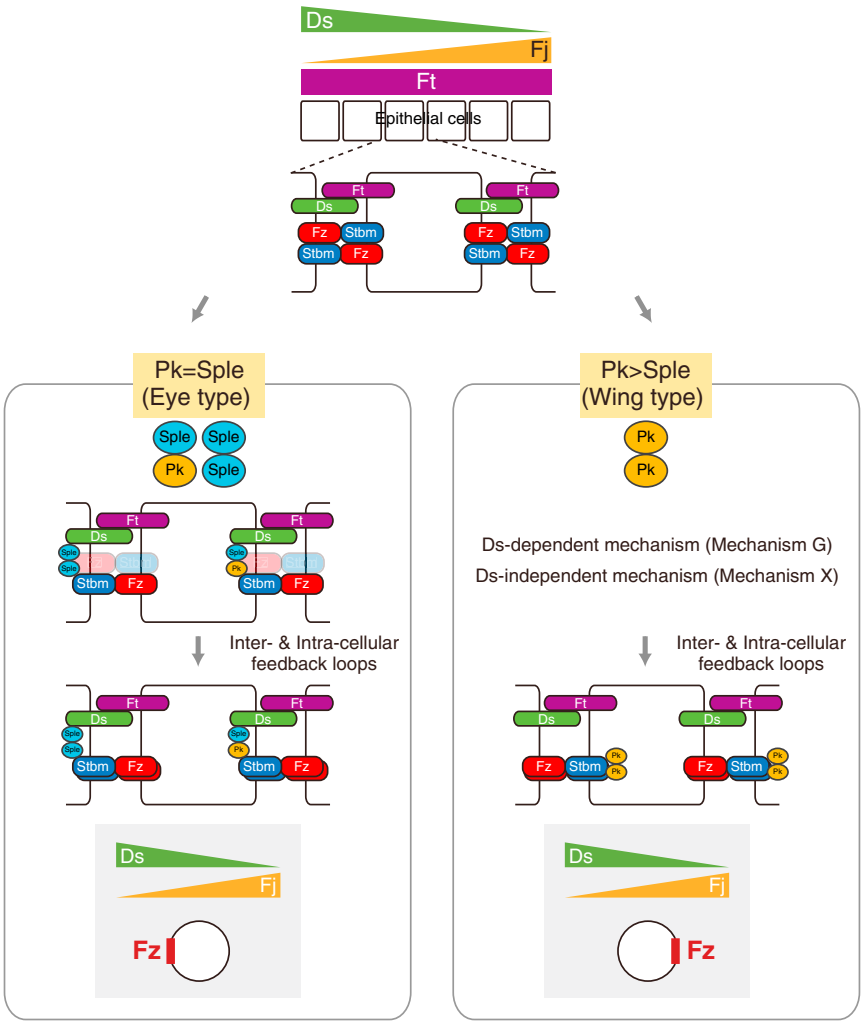

Figure 7. Model for the Role of the Pk:Sple Ratio in Determining PCP Core Protein Asymmetry Relative to the Ds/Ft Asymmetries

Top: in whole tissue, the Ds and Fj gradients initially co-operate with Ft, which is expressed uniformly across all cells in the tissue, to produce asymmetric binding of Ds and Ft at each cell boundary (refer to Figure S1B). At this point in time, the PCP core proteins do not exhibit prominent asymmetric localization within any cells. However, depending on the Pk:Sple ratio in a given tissue, the localization of PCP core proteins relative to the Ds-Ft asymmetries can adopt one of two polarities. See Discussion for more detail.

(1) whether and/or how Dachs is involved in Sple-Ds cooperation/interaction and (2) how Pk becomes engaged in Dachs function and vice versa.

Although our experiments do not directly reveal the molecular mechanism by which polarized Sple complexes regulate the asymmetry of the core proteins, we developed a mathematical model based on this study and previous studies by ourselves and others that supports the proposed mechanism governing the core protein asymmetry (see Supplemental Information; Figure 7). Our model includes a possible reaction where Sple stabilizes the membrane localization of Stbm on the cell edge with the highest Ds level (see Supplemental Information; Figure S3I). An alternative possibility is that, in addition to the above mechanism, Sple directly promotes the formation of the Fz asymmetry via reversing the direction of Fz transport, by changing the orientation of the microtubule array (Olofsson et al., 2014). Future work will include elucidating the molecular mechanism by which the Pk:Sple ratio regulates the core protein asymmetry, as well as determining how the Pk:Sple ratio is differentially regulated in various tissues.

EXPERIMENTAL PROCEDURES

Histological Analyses

UAS constructs were expressed using *pnr*-GAL4, *sd*-GAL4, *MS1096*-GAL4, *tub*-GAL4, *Dll*-GAL4, and *Actin* > CD2 > GAL4. Adult fly cuticles and wings were prepared using standard methods. Immunofluorescence experiments in pupal wings were performed using standard procedures. For clonal expression, Flp expression was induced by heat shock at 37°C for 40 min at 48–72 hr AEL, which excised the stop cassette from *Actin* > *stop* > EGFP-tagged genes. For ubiquitous expression using *Actin* > *stop* > EGFP-tagged genes, Flp expression was induced at 38°C for 2 hr at the indicated developmental stages, as previously described (Strutt and Strutt, 2002). Immunofluorescence staining of pupal wings and wing discs from third-instar larvae was performed using standard protocols.

qRT-PCR

Quantitative RT-PCR was performed using a standard protocol. Total RNA from larval eyes and wing discs (96 or 97 hr AEL) or pupal eyes and wings (15 hr APF) was extracted using the RNAqueous-Micro Kit (Ambion), and reverse transcription was performed using the Transcriptor First Strand cDNA Synthesis Kit (Roche). Quantitative RT-PCR was performed on a LightCycler480 (Roche) using LightCycler480 SYBR Green I Master (Roche).

SUPPLEMENTAL INFORMATION

Supplemental Information includes Supplemental Results, Supplemental Discussion, Supplemental Experimental Procedures, Supplemental Procedures for Mathematical Model, seven figures, and five movies and can be found with this article online at http://dx.doi.org/10.1016/j.celrep.2014.06.009.

AUTHOR CONTRIBUTIONS

T.A. and M.Y. designed and carried out the experiments. M.A. built the mathematical model and performed simulations with input from M.Y. and T.A. J.L.M.-W., T. Stoeger, J.A.K., and M.Y. contributed the initial analysis of the reversed PCP phenotype. J.S., H.S., T. Sasaki, and M.A. contributed to the image and statistic analyses. M.Y. wrote the paper together with T.A. and M.A.

ACKNOWLEDGMENTS

We thank D. Gubb, P. Adler, K. Irvine, D. Strutt, T. Uemura, F. Wirtz-Peitz, the Kyoto Stock Center, the Vienna Drosophila RNAi Center, the Bloomington Drosophila Stock Center, Drosophila Genomics Resource Center, Transgenic RNAi Project (TRiP), Developmental Studies of Hybridoma Bank (DSHB), and Addgene for fly stocks, antibodies, and plasmids and N. Odaka, M. Suzuki, and A. Kato for technical assistance. We thank Jeffrey D. Axelrod for communicating results before publication. This work was supported by Grant-in-Aid for Scientific Research on Innovative Areas from the Ministry of Education, Culture, Sports and Technology of Japan (MEXT); the Japan Society for the Promotion of Science (JSPS); Takeda Science Foundation; and The Uehara Memorial Foundation (to M.Y.). T.A. is supported by MEXT. Work in J.A.K.'s lab is supported by the Austrian Academy of Sciences, the Austrian Science Fund (FWF; grants I_552-B19 and Z_153_B09), and an advanced grant of the European Research Council (ERC). T. Sasaki is supported by MEXT, JSPS, and the Takeda Science Foundation and NEXT program. T. Sasaki and M.Y. were supported by the Global COE Program of MEXT.

Received: September 10, 2013
Revised: April 9, 2014
Accepted: June 5, 2014
Published: July 3, 2014

REFERENCES

Adler, P.N. (2002). Planar signaling and morphogenesis in Drosophila. Dev. Cell *2*, 525–535.

Adler, P.N., Charlton, J., and Liu, J. (1998). Mutations in the cadherin superfamily member gene dachsous cause a tissue polarity phenotype by altering frizzled signaling. Development *125*, 959–968.

Aigouy, B., Farhadifar, R., Staple, D.B., Sagner, A., Röper, J.C., Jülicher, F., and Eaton, S. (2010). Cell flow reorients the axis of planar polarity in the wing epithelium of Drosophila. Cell *142*, 773–786.

Ambegaonkar, A.A., Pan, G., Mani, M., Feng, Y., and Irvine, K.D. (2012). Propagation of Dachsous-Fat planar cell polarity. Curr. Biol. *22*, 1302–1308.

Amonlirdviman, K., Khare, N.A., Tree, D.R., Chen, W.S., Axelrod, J.D., and Tomlin, C.J. (2005). Mathematical modeling of planar cell polarity to understand domineering nonautonomy. Science *307*, 423–426.

Axelrod, J.D. (2001). Unipolar membrane association of Dishevelled mediates Frizzled planar cell polarity signaling. Genes Dev. *15*, 1182–1187.

Bastock, R., Strutt, H., and Strutt, D. (2003). Strabismus is asymmetrically localised and binds to Prickle and Dishevelled during Drosophila planar polarity patterning. Development *130*, 3007–3014.

Bosveld, F., Bonnet, I., Guirao, B., Tlili, S., Wang, Z., Petitalot, A., Marchand, R., Bardet, P.L., Marcq, P., Graner, F., and Bellaïche, Y. (2012). Mechanical control of morphogenesis by Fat/Dachsous/Four-jointed planar cell polarity pathway. Science *336*, 724–727.

Brittle, A.L., Repiso, A., Casal, J., Lawrence, P.A., and Strutt, D. (2010). Four-jointed modulates growth and planar polarity by reducing the affinity of dachsous for fat. Curr. Biol. *20*, 803–810.

Brittle, A., Thomas, C., and Strutt, D. (2012). Planar polarity specification through asymmetric subcellular localization of Fat and Dachsous. Curr. Biol. *22*, 907–914.

Casal, J., Lawrence, P.A., and Struhl, G. (2006). Two separate molecular systems, Dachsous/Fat and Starry night/Frizzled, act independently to confer planar cell polarity. Development *133*, 4561–4572.

Chae, J., Kim, M.J., Goo, J.H., Collier, S., Gubb, D., Charlton, J., Adler, P.N., and Park, W.J. (1999). The Drosophila tissue polarity gene starry night encodes a member of the protocadherin family. Development *126*, 5421–5429.

Chen, W.S., Antic, D., Matis, M., Logan, C.Y., Povelones, M., Anderson, G.A., Nusse, R., and Axelrod, J.D. (2008). Asymmetric homotypic interactions of the atypical cadherin flamingo mediate intercellular polarity signaling. Cell *133*, 1093–1105.

Clark, H.F., Brentrup, D., Schneitz, K., Bieber, A., Goodman, C., and Noll, M. (1995). Dachsous encodes a member of the cadherin superfamily that controls imaginal disc morphogenesis in Drosophila. Genes Dev. *9*, 1530–1542.

Classen, A.K., Anderson, K.I., Marois, E., and Eaton, S. (2005). Hexagonal packing of Drosophila wing epithelial cells by the planar cell polarity pathway. Dev. Cell *9*, 805–817.

Das, G., Reynolds-Kenneally, J., and Mlodzik, M. (2002). The atypical cadherin Flamingo links Frizzled and Notch signaling in planar polarity establishment in the Drosophila eye. Dev. Cell *2*, 655–666.

Das, G., Jenny, A., Klein, T.J., Eaton, S., and Mlodzik, M. (2004). Diego interacts with Prickle and Strabismus/Van Gogh to localize planar cell polarity complexes. Development *131*, 4467–4476.

Doyle, K., Hogan, J., Lester, M., and Collier, S. (2008). The Frizzled Planar Cell Polarity signaling pathway controls Drosophila wing topography. Dev. Biol. *317*, 354–367.

Feiguin, F., Hannus, M., Mlodzik, M., and Eaton, S. (2001). The ankyrin repeat protein Diego mediates Frizzled-dependent planar polarization. Dev. Cell *1*, 93–101.

Goodrich, L.V., and Strutt, D. (2011). Principles of planar polarity in animal development. Development *138*, 1877–1892.

Groth, A.C., Fish, M., Nusse, R., and Calos, M.P. (2004). Construction of transgenic Drosophila by using the site-specific integrase from phage phiC31. Genetics *166*, 1775–1782.

Gubb, D., and García-Bellido, A. (1982). A genetic analysis of the determination of cuticular polarity during development in Drosophila melanogaster. J. Embryol. Exp. Morphol. *68*, 37–57.

Gubb, D., Green, C., Huen, D., Coulson, D., Johnson, G., Tree, D., Collier, S., and Roote, J. (1999). The balance between isoforms of the prickle LIM domain protein is critical for planar polarity in Drosophila imaginal discs. Genes Dev. *13*, 2315–2327.

Harumoto, T., Ito, M., Shimada, Y., Kobayashi, T.J., Ueda, H.R., Lu, B., and Uemura, T. (2010). Atypical cadherins Dachsous and Fat control dynamics of noncentrosomal microtubules in planar cell polarity. Dev. Cell *19*, 389–401.

Hogan, J., Valentine, M., Cox, C., Doyle, K., and Collier, S. (2011). Two frizzled planar cell polarity signals in the Drosophila wing are differentially organized by the Fat/Dachsous pathway. PLoS Genet. *7*, e1001305.

Ishikawa, H.O., Takeuchi, H., Haltiwanger, R.S., and Irvine, K.D. (2008). Four-jointed is a Golgi kinase that phosphorylates a subset of cadherin domains. Science *321*, 401–404.

Jenny, A., Darken, R.S., Wilson, P.A., and Mlodzik, M. (2003). Prickle and Strabismus form a functional complex to generate a correct axis during planar cell polarity signaling. EMBO J. *22*, 4409–4420.

Jenny, A., Reynolds-Kenneally, J., Das, G., Burnett, M., and Mlodzik, M. (2005). Diego and Prickle regulate Frizzled planar cell polarity signalling by competing for Dishevelled binding. Nat. Cell Biol. *7*, 691–697.

Lawrence, P.A., Casal, J., and Struhl, G. (2004). Cell interactions and planar polarity in the abdominal epidermis of Drosophila. Development *131*, 4651–4664.

Lee, H., and Adler, P.N. (2002). The function of the frizzled pathway in the Drosophila wing is dependent on inturned and fuzzy. Genetics *160*, 1535–1547.

Ma, D., Yang, C.H., McNeill, H., Simon, M.A., and Axelrod, J.D. (2003). Fidelity in planar cell polarity signalling. Nature *421*, 543–547.

Mahoney, P.A., Weber, U., Onofrechuk, P., Biessmann, H., Bryant, P.J., and Goodman, C.S. (1991). The fat tumor suppressor gene in Drosophila encodes a novel member of the cadherin gene superfamily. Cell *67*, 853–868.

Mao, Y., Rauskolb, C., Cho, E., Hu, W.L., Hayter, H., Minihan, G., Katz, F.N., and Irvine, K.D. (2006). Dachs: an unconventional myosin that functions downstream of Fat to regulate growth, affinity and gene expression in Drosophila. Development *133*, 2539–2551.

Mao, Y., Kucuk, B., and Irvine, K.D. (2009). Drosophila lowfat, a novel modulator of Fat signaling. Development *136*, 3223–3233.

Matakatsu, H., and Blair, S.S. (2004). Interactions between Fat and Dachsous and the regulation of planar cell polarity in the Drosophila wing. Development *131*, 3785–3794.

Matakatsu, H., and Blair, S.S. (2008). The DHHC palmitoyltransferase approximated regulates Fat signaling and Dachs localization and activity. Curr. Biol. *18*, 1390–1395.

Mummery-Widmer, J.L., Yamazaki, M., Stoeger, T., Novatchkova, M., Bhalerao, S., Chen, D., Dietzl, G., Dickson, B.J., and Knoblich, J.A. (2009). Genome-wide analysis of Notch signalling in Drosophila by transgenic RNAi. Nature *458*, 987–992.

Olofsson, J., Sharp, K.A., Matis, M., Cho, B., and Axelrod, J.D. (2014). Prickle/Spiny-legs isoforms control the polarity of the apical microtubule network in PCP. Development http://dx.doi.org/10.1242/dev.105932.

Pfeiffer, B.D., Ngo, T.T., Hibbard, K.L., Murphy, C., Jenett, A., Truman, J.W., and Rubin, G.M. (2010). Refinement of tools for targeted gene expression in Drosophila. Genetics *186*, 735–755.

Rogulja, D., Rauskolb, C., and Irvine, K.D. (2008). Morphogen control of wing growth through the Fat signaling pathway. Dev. Cell *15*, 309–321.

Sagner, A., Merkel, M., Aigouy, B., Gaebel, J., Brankatschk, M., Jülicher, F., and Eaton, S. (2012). Establishment of global patterns of planar polarity during growth of the Drosophila wing epithelium. Curr. Biol. *22*, 1296–1301.

Shimada, Y., Usui, T., Yanagawa, S., Takeichi, M., and Uemura, T. (2001). Asymmetric colocalization of Flamingo, a seven-pass transmembrane cadherin, and Dishevelled in planar cell polarization. Curr. Biol. *11*, 859–863.

Shimada, Y., Yonemura, S., Ohkura, H., Strutt, D., and Uemura, T. (2006). Polarized transport of Frizzled along the planar microtubule arrays in Drosophila wing epithelium. Dev. Cell *10*, 209–222.

Simon, M.A. (2004). Planar cell polarity in the Drosophila eye is directed by graded Four-jointed and Dachsous expression. Development *131*, 6175–6184.

Simon, M.A., Xu, A., Ishikawa, H.O., and Irvine, K.D. (2010). Modulation of fat:dachsous binding by the cadherin domain kinase four-jointed. Curr. Biol. *20*, 811–817.

Simons, M., and Mlodzik, M. (2008). Planar cell polarity signaling: from fly development to human disease. Annu. Rev. Genet. *42*, 517–540.

Strutt, D.I. (2001). Asymmetric localization of frizzled and the establishment of cell polarity in the Drosophila wing. Mol. Cell *7*, 367–375.

Strutt, D.I. (2002). The asymmetric subcellular localisation of components of the planar polarity pathway. Semin. Cell Dev. Biol. *13*, 225–231.

Strutt, H., and Strutt, D. (2002). Nonautonomous planar polarity patterning in Drosophila: dishevelled-independent functions of frizzled. Dev. Cell *3*, 851–863.

Strutt, H., and Strutt, D. (2008). Differential stability of flamingo protein complexes underlies the establishment of planar polarity. Curr. Biol. *18*, 1555–1564.

Strutt, D., Johnson, R., Cooper, K., and Bray, S. (2002). Asymmetric localization of frizzled and the determination of notch-dependent cell fate in the Drosophila eye. Curr. Biol. *12*, 813–824.

Strutt, H., Thomas-MacArthur, V., and Strutt, D. (2013). Strabismus promotes recruitment and degradation of farnesylated prickle in Drosophila melanogaster planar polarity specification. PLoS Genet. *9*, e1003654.

Taylor, J., Abramova, N., Charlton, J., and Adler, P.N. (1998). Van Gogh: a new Drosophila tissue polarity gene. Genetics *150*, 199–210.

Tree, D.R., Shulman, J.M., Rousset, R., Scott, M.P., Gubb, D., and Axelrod, J.D. (2002). Prickle mediates feedback amplification to generate asymmetric planar cell polarity signaling. Cell *109*, 371–381.

Usui, T., Shima, Y., Shimada, Y., Hirano, S., Burgess, R.W., Schwarz, T.L., Takeichi, M., and Uemura, T. (1999). Flamingo, a seven-pass transmembrane cadherin, regulates planar cell polarity under the control of Frizzled. Cell *98*, 585–595.

Villano, J.L., and Katz, F.N. (1995). four-jointed is required for intermediate growth in the proximal-distal axis in Drosophila. Development *121*, 2767–2777.

Vinson, C.R., Conover, S., and Adler, P.N. (1989). A Drosophila tissue polarity locus encodes a protein containing seven potential transmembrane domains. Nature *338*, 263–264.

Wolff, T., and Rubin, G.M. (1998). Strabismus, a novel gene that regulates tissue polarity and cell fate decisions in Drosophila. Development *125*, 1149–1159.

Wu, J., and Mlodzik, M. (2008). The frizzled extracellular domain is a ligand for Van Gogh/Stbm during nonautonomous planar cell polarity signaling. Dev. Cell *15*, 462–469.

Wu, J., and Mlodzik, M. (2009). A quest for the mechanism regulating global planar cell polarity of tissues. Trends Cell Biol. *19*, 295–305.

Yang, C.H., Axelrod, J.D., and Simon, M.A. (2002). Regulation of Frizzled by fat-like cadherins during planar polarity signaling in the Drosophila compound eye. Cell *108*, 675–688.